(2)

AD-A247 089

DTIC
ELECTE
MAR 9 1992
S C D

INTRACELLULAR MEMBRANE AND SYNAPTIC PROPERTIES IN MEDIAL PREOPTIC SLICES CONTAINING THE SEXUALLY DIMORPHIC NUCLEUS OF THE RAT

Neil W. Hoffman, Yang I. Kim, Roger A. Gorski and F. Edward Dudek[1]

Mental Retardation Research Center
and
Laboratory of Neuroendocrinology
Brain Research Institute

UCLA Center for the Health Sciences
760 Westwood Plaza
Los Angeles, CA 90024-1759

[illegible] A
Approved for public release;
Distribution Unlimited

Running Head: Electrophysiology of medial preoptic neurons

Key Words: Medial Preoptic Area, Medial Preoptic Nucleus, Sexually Dimorphic Nucleus of Preoptic Area, Intracellular Recording, Biocytin, Low-threshold Ca^{2+} spikes, Gamma-Amino Butyric Acid

[1] To whom correspondence should be addressed

017

92-05773

Atch-9

SUMMARY AND CONCLUSIONS

1. Passive and active electrophysiological properties of neurons (n=46) in the medial preoptic area (MPOA) were studied in hypothalamic slices from rats (primarily males). This investigation evaluated whether the MPOA contains a heterogeneous population of cell types, defined on the basis of electrophysiological properties such as low-threshold Ca^{2+} spikes (LTS) and current-voltage (I-V) relations. Evoked and spontaneous synaptic potentials were also studied in these neurons. Electrical properties were compared between neurons in the sexually dimorphic nucleus of the preoptic area (SDN-POA) with those situated in other parts of the MPOA.

2. Biocytin-injected neurons (n = 24) were found in the SDN-POA, as well as other parts of the medial preoptic nucleus and MPOA. Stained neurons had 1 or 2 primary dendrites (46% of stained cells) or had multipolar dendritic arrays (54% of cells); dendrites were aspiny or sparsely spiny and displayed limited branching. Morphologically definable cell types were not specific to medial preoptic subdivisions.

3. In response to depolarization from a hyperpolarized condition, medial preoptic cells were uniformly capable of generating LTS potentials that generated one or more action potentials. In addition to being voltage dependent, these LTS potentials were time dependent and Ni^{2+} sensitive.

4. Other membrane properties were also similar between cells in different subdivisions of the MPOA, between medial preoptic neurons with differing morphology, and between stained and unstained cells. Most neurons (92%) displayed linear I-V relations in the

Accession
NTIS GRA&
DTIC TAB
Unannounced
Justificati
By
Distribution/
Availability
Dist Avail and
Special
A-1
DTIC
COPY
INSPECTED
6

hyperpolarizing direction. Only two cells showed evidence for weak anomalous inward rectification at hyperpolarized membrane potentials. Average values for the resting potential of medial preoptic neurons ($\pm$ SEM) was -60.7 $\pm$ 2.2 mV; for input resistance, 196 $\pm$ 20 MΩ; and for membrane time constant, 15.2 $\pm$ 2.5 ms.

5. The typical response to depolarizing current pulses delivered at or near resting potential was a train of Na^+ spikes, the frequency of which was directly related to current-pulse intensity. Spike trains displayed moderate spike-frequency adaptation; however, the degree of adaptation was variable across neurons. Afterhyperpolarizations usually followed spike trains.

6. Spontaneous postsynaptic potentials (PSPs), most of which were inhibitory, were frequently recorded. In most medial preoptic neurons (83%), extracellular stimulation of the dorsal preoptic region evoked a fast EPSP closely followed by an IPSP. In some neurons, evoked EPSPs were not observed unless the evoked IPSPs were blocked with 10-50 μM bicuculline. The IPSPs reversed at -71 $\pm$ 5 mV (i.e., near E_{Cl^-} reported for other hypothalamic neurons).

7. These findings indicate that the MPOA is predominantly composed of neurons that, despite having differing morphology, share similar electrophysiological properties. Although electrophysiological properties varied to some extent across neurons, sets of properties did not appear to covary, and thus clearly recognizable cell types were not apparent in this region. The prevalence of such properties as LTS potentials and synaptic inhibition may have relevance for physiological functions associated with this sexually dimorphic region of the hypothalamus.

INTRODUCTION

The medial preoptic area (MPOA) is a hypothalamic region with a role in regulating diverse physiological processes, including fluid volume (Swanson and Mogenson 1981; van Gemert et al. 1975), core temperature (Boulant 1980), and reproduction (Giontonio et al. 1970; see Gorski 1985). The firing rates of medial preoptic neurons are sensitive to osmotic stimuli, glucose, temperature changes, and gonadal steroids (Boulant and Silva 1989). Lesions of the MPOA prevent phasic patterns of gonadotropic hormonal activity that promote ovulation in rodents (see Gorski 1985) and also reduce male sexual (Giontonio et al. 1970) and maternal (Cohn and Gerall, 1989; Jacobson et al., 1980) behaviors. For these reproductive activities to occur during adulthood, the presence of particular gonadal steroids during critical periods in development is necessary (see Gorski 1985). Gonadal steroids also alter anatomical structures within the MPOA, including a category of spine synapses (Raisman and Field 1973) and the size of cytoarchitectonic subdivisions. For example, the phenotypic expression of the larger male version of the sexually dimorphic nucleus of the preoptic area (SDN-POA) (Gorski et al. 1980) requires circulating androgens perinatally (Jacobson et al. 1981). However, it is unknown how steroids affect neuronal electrical properties during the development of this region or during adulthood.

Anatomical and neurochemical techniques have been used extensively to study the MPOA from neuroendocrine and developmental perspectives. The animal model for most of this work has been the rat. In this species the MPOA is an anatomically complex region that comprises several subdivisions, including three subdivisions of the medial preoptic

nucleus, the largest and most pronounced cell-dense region of the MPOA. One of these subdivisions, the medial preoptic nucleus centralis, largely corresponds with the posterior SDN-POA (Block and Gorski 1988; Simerly and Swanson 1986). The MPOA contains several types of cells that synthesize a wide variety of neurotransmitters and peptides. Medial preoptic neurons stain positively for such hypophysiotropic substances as luteinizing hormone-releasing hormone, corticotropin-releasing factor, thyrotropin-releasing hormone, and somatostatin, as well as other neuroactive peptides (Simerly et al. 1986). Whether these anatomical characteristics of the MPOA are associated with a heterogeneity of cell types, each defined by a specific set of electrophysiological properties, is presently unknown.

In other hypothalamic nuclei, correlations between anatomical characteristics and electrophysiological properties have been observed. For example, three categories of ventromedial neurons, each possibly subserving a separate biological function, were identified on the combined basis of their intracellular electrical properties and neuronal morphology (Minami et al. 1986a and b). Also, in the region of the paraventricular nucleus of the rat, magnocellular neurons, parvocellular neurons, and cells surrounding the nucleus were found to have distinct and identifying membrane properties. These included the capacity for low-threshold Ca^{2+} spikes (LTS) and the linearity versus nonlinearity of current-voltage (I-V) relations (Hoffman et al. 1991; Tasker and Dudek 1991). The intrinsic electrophysiological properties of paraventricular magnocellular neurons are similar to magnocellular neurons in the supraoptic nucleus (Andrew and Dudek 1983; Andrew and Dudek 1984a and b; Bourque and Renaud 1985). The two subpopulations of supraoptic magnocellular neurons, defined by their synthesis of oxytocin or vasopressin, share qualitatively similar intrinsic

properties despite their different aggregate firing characteristics in vivo (see Poulain and Wakerly 1982). Therefore, the MPOA may be comprised of cell types with distinct intrinsic membrane properties that relate to specific biological functions, or it may contain a single cell type defined by a common set of intrinsic properties. With either situation, these electrophysiological properties would provide the substrate for integrating specific neuronal inputs or neurohumoral conditions that control physiological processes. Gonadal steroids may regulate these electrophysiological properties through relatively permanent organizational effects during development or through more transient activational effects during adulthood (see Arnold 1990; Naftolin 1981). Steroid-induced changes in the electrical properties of medial preoptic neurons also may be associated with sex differences in reproductive processes and anatomical characteristics.

Gamma-aminobutyric acid (GABA) is likely to be the dominant inhibitory transmitter throughout the hypothalamus (van den Pol et al. 1990). Spontaneous and evoked IPSPs that are mediated by GABA have been identified in other hypothalamic regions, including the paraventricular (Tasker and Dudek, in preparation), supraoptic (Randle et al. 1986), and suprachiasmatic (Kim and Dudek, 1990) nuclei. GABA may also be important for functions attributed to the MPOA and may mediate inhibitory synaptic transmission in this area. Regional GABA concentration is relatively high in the MPOA (Mansky et al. 1982), and many medial preoptic neurons stain for the GABA-synthesizing enzyme, glutamate decarboxylase (Flügge et al. 1986). GABA neurons in the MPOA may provide an important link in the feedback actions of gonadal steroids on the release of gonadotropic hormones and prolactin from the anterior pituitary (Jarry et al. 1991). These findings suggest that

inhibitory synaptic contacts are wide-spread throughout the MPOA, although this has yet to be shown in intracellular recordings from this region in the rat.

Little information is available regarding precise intrinsic and synaptic electrical properties of neurons in the MPOA and how these properties may vary across medial preoptic subdivisions. A recent report (Hodgkiss and Kelly 1990) of intracellular recordings from medial preoptic neurons in the mouse has appeared, but the focus of this study was to compare grafted preoptic cells with normal (control) neurons in tissue slices. LTS potentials were identified in a proportion of these cells; however, precise cytoarchitectural sites of recordings were not determined histologically . Another group recently recorded intracellularly from thermosensitive neurons in the medial preoptic area-anterior hypothalamus of the rat (Curras et al. 1991). However, the locations of these recordings were not determined histologically, and the presence or absence of LTS potentials was not investigated. These issues are important since gonadal steroids could alter specific intrinsic (e.g., LTS) and synaptic (e.g., GABA-mediated IPSPs) properties of a select cell type(s) specific to a subdivision such as the SDN-POA. Therefore, by combining intracellular recording with intracellular staining and histology, we tested three hypotheses: (1) Neurons in the SDN-POA are electrophysiologically homogeneous but differ from cells elsewhere in the medial preoptic nucleus and MPOA; (2) specific types of medial preoptic neurons generate LTS potentials; (3) GABA-mediated synaptic inhibition is wide-spread among these cells. Our results indicate that the MPOA mostly contains a homogeneous set of neurons with the capacity for LTS potentials and that GABA-mediated IPSPs are consistently recorded in these cells. This study is an initial step toward examining developmental and

activational influences of gonadal steroids on the electrical properties of cells residing in sexually dimorphic brain regions. Part of these data has been presented in abstract form (Hoffman et al. 1990).

METHODS

Slice Preparation

Hypothalamic slices containing the MPOA were obtained from adult Sprague-Dawley rats (150-300 g, Charles Rivers Breeding Laboratory) during the light phase of a 12 hr light/dark cycle. Animals were anesthetized with nembutal (100 mg/kg IP), decapitated, and their brains quickly removed and placed in chilled (1-4°C), oxygenated, artificial cerebrospinal fluid (ACSF). This consisted (in mM) of 124 NaCl, 26 $NaHCO_3$, 3 KCl, 1.3 $MgSO_4$, 1.4 NaH_2PO_4, 2.4 $CaCl_2$, and 11 glucose. A tissue block containing the hypothalamus was dissected and sectioned coronally at 400 μm on a vibroslice (Campden Instruments). The anterior commissure, optic chiasm, and third ventricle provided landmarks for identifying the MPOA in a tissue slice. Slices containing the MPOA (see Fig. 1) were placed in a ramp-type recording chamber, where a humidified mixture of 95% O_2 and 5% CO_2 interfaced with the perfused ACSF (pH 7.4; 34 $\pm$ 1°C). Before the start of experiments, slices were allowed to equilibrate in the recording chamber for 2-3 h.

Electrophysiological Techniques

Micropipettes for intracellular recording were pulled from glass capillaries (1.0 mm OD, 0.5 mm ID, American Glass Co.), using a Flaming-Brown puller; they were filled with either 2 M K-acetate or 2 M K-acetate containing 2% biocytin (Sigma) and had tip resistances of 90-200 MΩ. Microelectrodes were advanced through slices in 4-μm steps with a piezoelectric microdrive (Nanostepper), and cell impalements were achieved by oscillating

the negative-capacitance feedback of an intracellular electrometer. Electrical signals were recorded with the electrometer (Model IR183, Neurodata Instruments or Axoclamp-2A, Axon Instruments), which contained a bridge circuit. Signals were stored on video cassettes, using an analogue to digital converter (Neurocorder Model DR-484, Neurodata Instruments), and traces were generated (ISC67AVE system, RC Electronics) and printed on an X-Y plotter or a laser printer.

Stimulating electrodes were made from insulated platinum-iridium wire (diameter=75 μm). Constant-current stimulation was applied extracellularly to the dorsal preoptic region (see Fig. 1) in a series of intensities (5-700 μA, 0.5 ms, 0.3 Hz) to evoke a complete range of synaptic responses. This stimulation site was chosen because it contains afferents to the medial preoptic nucleus (Simerly and Swanson 1986) and because stimulation applied to this site consistently elicited synaptic responses in recorded neurons.

Drug Application

In some experiments bicuculline methiodide (10 and 50 μM) was added to the ACSF perfusate to test whether IPSPs were mediated by $GABA_A$ receptors. Fast Na^+ spikes were blocked with bath applications of tetrodotoxin (TTX) (50 μg/ml). Ca^{2+} potentials were identified by replacing the standard perfusate with one containing (in mM) 125.5 NaCl, 3 KCl, 1.3 $MgCl_2$, 10 N-2-hydroxyethylpiperazine-N'-2-ethanesulphonic acid (HEPES), 11 glucose, 0.2 CaCl2 and 0.5 $NiCl_2$.

Anatomy

Biocytin was iontophoresed intracellularly, and injected cells were then histologically processed as previously described (Horikawa and Armstrong 1988; Tasker et al. 1991). Briefly, slices were immersion-fixed for at least 12 hr in 4% paraformaldehyde in 0.1 M Na-cacodylate buffer (pH 7.25; 5°C) and sectioned on a sliding microtome. An avidin-biotinylated horseradish peroxidase bridge was attached (Vectastain Elite kit, Vector Laboratories) and an opaque reaction product formed using a glucose-oxidase procedure and diaminobenzidine(-4HCl) (Sigma) as the chromogen (Smithson et al. 1984). Sections were mounted onto gelatin-coated slides and counterstained with cresol violet or toluene blue.

RESULTS

General Electrophysiological Properties

Data were from intracellular recordings of 46 medial preoptic neurons, all of which had overshooting action potentials $\geq$ 50 mV measured from threshold to peak (mean $\pm$ SEM = 61.2 $\pm$ 1.6 mV) and apparent resting potentials at or more negative than -50 mV (mean = -60.7 $\pm$ 2.2 mV, where each resting potential could be verified at the end of an experiment, n = 33). All recordings included in this study were stable for at least 10 min. Most of the recordings (94%) were made in slices from males; however, 3 medial preoptic neurons from ovariectomized females were included in analyses of LTS potentials, which were similar to those recorded in male tissue. Figure 1 is a schematic of the coronal slice preparation used in these experiments.

Insert Fig. 1 about here.

Medial Preoptic Subdivisions and Neuronal Morphology

Twenty four neurons were recovered after impalement with biocytin-filled electrodes and subsequent histological procedures; these cells were situated in the SDN-POA, the medial preoptic nucleus medialis (MPNm), and elsewhere in the MPOA. Stable recordings were obtained in 18 of these cells (see Table 1). Neurons varied with respect to their dendritic arbor: one set of cells (46% of stained neurons) had 1 or 2 primary dendrites (Fig. 2), and another set (54%) had multipolar dendritic arrays (Fig. 3). However, these

morphological characteristics were not uniquely associated with specific medial preoptic subdivisions examined in the present study (Fig. 4). Soma sizes were similar in both sets of neurons: longest-axis soma diameters of neurons with 1 or 2 primary dendrites ranged from 11 to 34 μm and shortest-axis diameters from 10 to 22 μm. Soma diameters of multipolar cells ranged from 16 to 34 μm (longest axis) and from 10 to 16 μm (shortest axis). Dendritic arbors in both sets of neurons were sparsely spiny or aspiny; only primary dendrites were observed on 38% of stained cells and both primary and secondary dendrites on 62% of the cells. Axons typically originated from primary dendrites and most often coursed in a medial to ventromedial direction (7 of 10 observations), in some cases giving off local collaterals (Fig. 5). Both primary axons and local collaterals contained varicosities (Figs. 2, 3 and 5). Regardless of cytoarchitectonic location or morphological appearance, stained neurons had similar electrical properties that did not differ from those recorded in most unstained (or non-anatomically recovered) neurons (see Table 1 and below).

Insert Figs. 2, 3, 4 and 5 about here

Insert Table 1 about here

Low-Threshold Potentials

The most salient intrinsic property of medial preoptic neurons was their capacity for low-threshold potentials, as observed in 98% of all recorded cells (n=46) and 100% of those neurons that were stained and histologically identified within medial preoptic subdivisions. In these cells a depolarization from a hyperpolarized condition produced an active

depolarization to Na^+-spike threshold, typically generating one or more (up to 3) action potentials. Low-threshold potentials were revealed by hyperpolarizing medial preoptic neurons and then superimposing a depolarizing current pulse (Fig. 6A and B). These potentials were also observed in the form of anode-break spikes following the offset of hyperpolarizing current pulses (Fig. 6C and D). Varying the duration of the hyperpolarizing current-pulse revealed that voltage-dependent deinactivation of the low-threshold conductance was also time dependent (Fig. 6C). The low-threshold potentials persisted during tetrodotoxin (TTX) block of fast, voltage-dependent Na^+ channels (n=1) (Fig. 6A and C, Fig. 7) but were blocked by bath application of Ni^{2+} in low Ca^{2+} HEPES buffer (n=3) (Fig. 7). Therefore, these events appear to be LTS potentials, as originally described in other central regions (Jahnsen and Llinás 1984).

In some medial preoptic neurons, LTS potentials appeared to underly oscillating membrane potentials, which followed the offset of hyperpolarizing current pulses and resultant anode-break spikes (Fig 6D). These oscillations were not observed in all cells.

Insert Figs. 6 and 7 about here.

Other Membrane Responses to Current Injections

Along with LTS potentials, medial preoptic neurons were similar in terms of other membrane properties. Most plots of I-V relations were linear, with little or no evidence of voltage- and time-dependent inward rectification at hyperpolarizing potentials up to and greater than 40 mV below resting potential (n=25) (Figure 8A and 8B, left). The hyperpolarizing I-V relations of only two neurons suggested inward rectification, and the I-V

plots from these cells were only weakly curvilinear (Figure 8B, right). One of these neurons had similar electrophysiological properties to other recorded cells in this study; however, the other cell was the only recorded neuron that displayed evidence for an A current and failed to generate an obvious LTS potential (data not shown). This neuron was not injected with biocytin, and so its position within the MPOA could not be verified.

Membrane time constants were derived from averaged voltage deflections (n=5-30) in response to weakly negative current pulses (50-100 pA). Input resistances were also calculated from these voltage transients. Time constants were computed from the charging portion of the voltage transient rather than from the discharging portion, which often reflected active membrane properties. Values for membrane time constants were calculated as previously described (Tasker and Dudek 1991). Briefly, points were taken at 0.3 ms intervals and plotted against time on a semilogarithmic scale; points were plotted as V_o-$V_t)/V_o$, where V_t = voltage at a given point and V_o = maximum voltage deflection. The linear portion of the resulting curve was fit by linear regression, the slope providing the value for the membrane time constant (Fig. 9). Medial preoptic neurons had a mean membrane time constant ($\pm$ SEM) of 15.2 $\pm$ 2.5 ms (n=23).

Depolarizing current pulses of different intensities were applied to evaluate repetitive firing properties of medial preoptic cells (n=21). In most neurons (88%) spike frequency increased as a function of current intensity, spike amplitude and frequency diminishing as a function of time during the pulse (thus showing spike-frequency adaptation) (Fig. 10). However, the degree of adaptation was variable across neurons, and only one or two action potentials could be evoked in 2 cells. In most neurons (83% of 24 cells), relatively small

afterhyperpolarizations followed spike trains (following 7-11 spikes, mean ± SEM amplitude = -4.7 ± 0.5 mV; duration = 64 ± 13 ms, measured at half maximum amplitude) (Fig. 10).

Insert Figs 8, 9, and 10 about here.

Synaptic Responses

Extracellular stimulation (50-700 μA) of the dorsal preoptic region (Fig. 11) reliably evoked synaptic potentials in recorded neurons (n=34). In most cells (73%) this stimulation produced a fast EPSP that was attenuated by a fast IPSP (Fig. 11A, Fig. 12A and B). The evoked IPSP were most often of short latency (Fig. 11A), although multiple IPSPs with different latencies were occasionally observed (Fig 11A, top trace, and B). In some instances spikes occurred at the termination of large IPSPs (Fig. 11B), suggesting that the IPSPs deinactivated the conductance underlying the LTS potentials. Spontaneous PSPs were frequently recorded, and among these events IPSPs were prominent (Fig. 11C). The mean reversal potential (± SEM) of evoked IPSPs was -71 ± 5 mV (n=7) (Fig. 12A), and bath application of bicuculline (10 and 50 μM) blocked the evoked IPSPs. In three neurons in which stimulation usually evoked only IPSPs in normal medium, bicuculline blocked the IPSPs and revealed EPSPs (Fig. 12B).

Insert Figs. 11 and 12 about here.

DISCUSSION

Homogeneity of Cells

A major aim of these experiments was to evaluate if medial preoptic neurons were heterogeneous or homogeneous in terms of their intrinsic electrophysiological properties. We specifically sought to determine if the subsets of cells residing in the SDN-POA and other medial preoptic subdivisions represent distinct classes or types of cells on the basis of intrinsic or synaptic properties. The hypothesis that the SDN-POA contains neurons with unique electrophysiological properties was not confirmed. Instead, it appears that the MPOA comprises neurons with a common set of electrophysiological properties and that these neurons form the dominant (or only) cell type across medial preoptic subdivisions. Unstained neurons, whose precise cytoarchitectonic locations could not be determined, also had properties similar to those of stained cells with verified locations within the MPOA. Among these cells, the lack of covariations among sets of examined electrophysiological properties indicated electrophysiological homogeneity. It is unlikely that the homogeneity reflects selection of cells residing in a single location or having a common morphology, because the intracellular staining confirmed that the data were obtained from a variety of locations and cells with differing morphology. Only one neuron failed to generate an obvious LTS potential; unlike all other recorded cells it also displayed an apparent A current (see Llinás 1988), and unlike all but one other medial preoptic neuron it displayed inward rectifying I-V relations in the hyperpolarizing direction. Although the position of this atypical cell within the MPOA was not histologically verifiable, this recording suggests the

possibility of a *small subset* of medial preoptic neurons with distinctly different properties from the majority of cells in this region.

LTS

As hypothesized, LTS potentials were generated by medial preoptic neurons, but these potentials did not differentiate cell types in this region. Unlike the paraventricular, ventromedial, and arcuate nuclei (Hoffman et al. 1991; Loose et al. 1990; Minami et al. 1986 a and b; Tasker and Dudek 1991), where only subsets of neurons display LTS potentials, all anatomically identified medial preoptic neurons recorded in the present investigation showed these potentials. This was also true for all but one unstained neuron. This finding appears to contrast with previous recordings from grafted and non-grafted medial preoptic neurons in mice, in which a large proportion of neurons were not identified as having LTS potentials (Hodgkiss and Kelly 1990). This apparent discrepancy could reflect a species difference or instead the different focus of the previous study (Hodgkiss and Kelly 1990). The LTS potentials recorded in the present study appeared to have a voltage dependence similar to that reported for cells in the inferior olivary nucleus (Llinás and Yarom 1981), thalamus (Jahnsen and Llinás 1984), and paraventricular (Hoffman et al. 1991; Tasker and Dudek 1991) and ventromedial (Minami et al. 1986 a and b) hypothalamic nuclei; they were similarly Ca^{2+} dependent in that they were blocked by bath application of Ni^{2+} in a low Ca^{2+}-containing medium. These data, plus the voltage dependence of these potentials, suggests that they are mediated by channel openings responsible for transient (T) currents, which, among Ca^{2+} channel types, are particularly sensitive to Ni^{2+} (Fox et al. 1987). In

medial preoptic neurons LTS potentials generated only one or a few Na^+ spikes and, in this respect, resembled hypothalamic parvocellular (type II) neurons in the paraventricular nucleus (Hoffman et al. 1991; Tasker and Dudek 1991). As recorded in paraventricular parvocellular neurons, LTS-mediated anode-break spikes in medial preoptic neurons could trigger membrane oscillations. However, these oscillations were not as robust as those reported for cells situated near but outside the paraventricular nucleus (type III neurons) (Hoffman et al. 1991; Tasker and Dudek 1991). Other membrane properties described below also indicate similarities between medial preoptic and paraventricular parvocellular neurons.

Other Intrinsic Properties

Values for input resistance, membrane time constant, Na^+ spike amplitude and duration, and resting potential were similar among medial preoptic neurons. Most medial preoptic cells had linear I-V relations in the hyperpolarizing direction, with the I-V plots from two cells deviating slightly from linearity. Similar values and I-V relations were reported for paraventricular parvocellular neurons (Hoffman et al. 1991; Tasker and Dudek 1991). This suggests two main points: (1) a broad category of hypothalamic parvocellular neurons with a common set of intrinsic electrophysiological properties extends across certain hypothalamic regions, and (2) these properties are important for integrating responses to the several homeostatic stimuli known to affect the activity of cells in this region (Boulant and Silva 1989).

Fast Synaptic Events and GABA

Findings from this study support the hypothesis that medial preoptic neurons receive fast, GABA-mediated synaptic inhibition. Spontaneous EPSPs and IPSPs were consistently recorded in these cells, and an EPSP-IPSP sequence could often be evoked by applying certain stimulus intensities to the dorsal preoptic region. The evoked IPSPs typically reduced the amplitude and duration of the evoked EPSPs, and, in some experiments, evoked EPSPs could be observed only when the IPSPs were blocked with bicuculline. This effect of bicuculline on IPSPs, coupled with an IPSP reversal near the Cl^- equilibrium potential (Randle et al. 1986), indicates that ligand-binding at $GABA_A$ receptors mediates these events. Previous findings suggest that GABA is synthesized by medial preoptic cells (Mansky et al. 1982; Flügge et al. 1986) and that GABA-releasing neurons participate in synchronizing phasic gonadotropic activity (Jarry et al. 1991). Our findings relate to this latter possibility in two ways: (1) GABA appears to be the primary, if not the only, neurotransmitter mediating fast IPSPs recorded in medial preoptic neurons; (2) the axons of stained cells often ramified into an apparent network of local collaterals, possibly forming local circuits for synchronizing activity in this region.

Future Direction

Properties frequently encountered in medial preoptic recordings (e.g., LTS potentials and $GABA_A$-receptor-mediated synaptic inhibition) probably play a significant role in interneuronal communication in this region of the hypothalamus. Conceivably, these electrophysiological properties could be regulated by testicular hormones that

developmentally regulate anatomical characteristics of the MPOA (Gorski et al. 1980; Jacobson et al. 1981; Raisman and Field 1973). Developmental studies and comparisons between males and females are required to assess possible electrophysiological "sexual dimorphism" and its regulation by gonadal steroids.

We thank Dr. P. Micevych for his advice and for the use of his histological specimens, both of which facilitated cytoarchitectural identifications. We also thank Dr. D. Birt for computer programming. The assistance of S. Sampogna and G. Allen in histologically processing tissue samples is gratefully acknowledged, as is the help provided by S. Belkin and C. Gray in preparing figures. This research was supported by a grant from the Air Force Office of Scientific Research to F. E. Dudek and a National Institutes of Health postdoctoral fellowship to N.W. Hoffman.

REFERENCES

Andrew, R.D., and Dudek, F.E. Burst discharge in mammalian neuroendocrine cells involves an intrinsic regenerative mechanism. *Science* 221: 1050-1052, 1983.

Andrew, R.D., and Dudek, F.E. Analysis of intracellularly recorded phasic bursting by mammalian neuroendocrine cells. *J. Neurophysiol.* 51: 552-566, 1984a.

Andrew, R.D., and Dudek, F.E. Intrinsic inhibition in magnocellular neuroendocrine cells of rat hypothalamus. *J. Physiol.* 353: 171-185, 1984b.

Arnold, A.P. Hormonally induced synaptic reorganization in the adult brain. In: *Hormones, Brain and Behavior in Vertebrates. 1. Sexual differentiation, neuroanatomical aspects, neurotransmitters and neuropeptides. Comp. Physiol.*, Basel: Karger, 1990, p. 82-91.

Bloch, G.J., and Gorski, R.A. Cytoarchitectonic analysis of the SDN-POA of the intact and gonadectomized rat. *J. Comp. Neurol.* 275: 604-612, 1988.

Boulant, J.A. Hypothalamic control of thermoregulation: neurophysiological basis. In: *Handbook of the Hypothalamus* 3 (part A), edited by P.J. Morgane and J. Panksepp. New York: Dekker, 1980, p. 1-82.

Boulant, J.A., and Silva, N.L. Multisensory hypothalamic neurons may explain interactions among regulatory systems. *News in Physiological Sciences* 4: 245-248, 1989.

Bourque, C.W., and Renaud, L.P. Calcium-dependent action potentials in rat supraoptic neurosecretory neurons recorded in vitro. *J. Physiol.* 363: 419-428, 1985.

Cohn, J., and Gerall, A.A. Pre- and postpuberal medial preoptic area lesions and maternal behavior in the rat. *Physiol. Behav.* 46: 333-336, 1989.

Curras, M.C., Kelso, S.R., and Boulant, J.A. Intracellular analysis of inherent and synaptic activity in hypothalamic thermosensitive neurons in the rat. *J. Physiol.* 440: 257-271, 1991.

Flügge, G., Oertel, W.H., and Wuttke, W. Evidence for estrogen-receptive GABAergic neurons in the preoptic/anterior hypothalamic area of the rat brain. *Neuroendocrinology* 53: 261-267, 1986.

Fox, A.P., Nowycky, M.C., Tsien, R.W. Kinetic and pharmacological properties distinguishing three types of calcium currents in chick sensory neurons. *J. Physiol.* 394: 149-172, 1987.

Giantonio, G.W., Lund, N.L., and Gerall, A.A. Effect of diencephalic and rhinencephalic lesions on the male rat's sexual behavior. *J. Comp. Physiol. Psychol.* 73: 38-46, 1970.

Gorski, R.A. Sexual dimorphisms of the brain. *J. Animal Sci.* 61: 38-61, 1985.

Gorski, R.A. Sexual differentiation of the brain: a model for drug-induced alterations of the reproductive system. *Environmental Health Perspectives* 70: 163-175, 1986.

Gorski, R.A., Harlan, R.E., Jacobson, C.D., Shryne, J.E., and Southam, A.M. Evidence for the existence of a sexually dimorphic nucleus of the preoptic area. *J. Comp. Neurol.* 193: 529-539, 1980.

Hodgkiss, J.P., and Kelly, J.S. An intracellular study of grafted and *in situ* preoptic area neurones in brain slices from normal and hypogonadal mice. *J. Physiol.* 423: 111-135, 1990.

Hoffman, N.W., Kim, Y.I., Gorski, R.A., and Dudek, F.E. Electrical and morphological characteristics of neurons in the male sexually dimorphic nucleus (SDN) of the rat medial preoptic area (MPOA). *Soc. Neurosci. Abstr.* 16: 574, 1990.

Hoffman, N.W., Tasker, J.G., and Dudek, F.E. Immunohistochemical differentiation of electrophysiologically defined neuronal populations in the region of the rat hypothalamic

paraventricular nucleus. *J. Comp. Neurol.* 307: 405-416, 1991.

Horikawa, K., and Armstrong, W.E. A versatile means of intracellular labeling: Injection of biocytin and its detection with avidin conjugates. *J. Neurosci. Methods* 25: 1-11, 1988.

Jacobson, C.D., Csernus, V.J., Shryne, J.E., and Gorski, R.D. The influence of gonadectomy, androgen exposure, or gonadal graft in the neonatal rat on the volume of the sexually dimorphic nucleus of the preoptic area. *J. Neurosci.* 1: 1142-1142, 1981.

Jacobson, C.D., Terkel, J., Gorski, R.A., and Sawyer, C.H. Effects of small medial preoptic area lesions on maternal behavior: retrieval and nest building in the rat. *Brain Res.* 194: 471-478, 1980.

Jahnsen, H., and Llinás, R. Electrophysiological properties of guinea-pig thalamic neurons: An *in vitro* study. *J. Physiol.* 349: 205-226, 1984.

Jarry, H., Leonhardt, S., Wuttke, W. Gamma-aminobutyric acid neurons in the preoptic/anterior hypothalamic area synchronize the phasic activity of the gonadotropin-releasing hormone pulse generator in ovariectomized rats. *Neuroendocrinology* 53: 261-267, 1991.

Kim, Y.I., and Dudek, F.E. Suprachiasmatic nucleus (SCN) neurons receiving retinal inputs are under the control of gamma-amino butyric acid (GABA). *Soc. Neurosci. Abstr.* 16: 574, 1990.

Llinás, R. R. The intrinsic electrophysiological properties of mammalian neurons: insights into central nervous system function. *Science* 242: 1654-1664, 1988.

Llinás, R., and Yarom, Y. Electrophysiology of mammalian inferior olivary neurons *in vitro*. Different types of voltage-dependent conductances. *J. Physiol.* 315: 549-567, 1981.

Loose, M.D., Ronnekleiv, O.K., and Kelly, M.J. Membrane properties and response to opioids of identified dopamine neurons in the guinea pig hypothalamus. *J. Neurosci.* 10: 3627-3634, 1990.

Mansky, T. Mestres-Ventura, P. and Wuttke, W. Involvement of GABA in the feedback action of estradiol on gonadotropin and prolactin release: hypothalamic GABA and catecholamine turnover rates. *Brain Res.* 231:353-364, 1982.

Minami, T., Oomura, Y., and Sugimori, M. Electrophysiological properties and glucose responsiveness of guinea-pig ventromedial hypothalamic neurones *in vitro*. *J. Physiol.* 380: 127-143: 1986a.

Minami, T., Oomura, Y., and Sugimori, M. Ionic basis for the electroresponsiveness of guinea-pig hypothalamic neurones *in vitro*. *J. Physiol.* 380: 145-156, 1986b.

Naftolin, F. Understanding the basis of sex differences. *Science* 211: 1263-1264, 1981.

Palkovits, M., and Brownstein, M.J. *Maps and Guide to MIcrodissection of the Rat Brain* Elsevier: New York, 1988.

Poulain, D.A., and Wakerley, J.B. Electrophysiology of hypothalamic magnocellular neurons secreting oxytocin and vasopressin. *Neuroscience* 7: 773-808, 1982.

Raisman, G. and Field, P.M. Sexual dimorphism in the neuropil of the preoptic area of the rat and its dependence on neonatal androgen. *Brain Res.* 54: 1-29, 1973.

Randle, J.C., Bourque, C.W., and Renaud, L.P. Characterization of spontaneous and evoked inhibitory postsynaptic potentials in rat supraoptic neurosecretory neurons in vitro. *J. Neurophysiol.* 56: 1703-1717, 1986.

Simerly, R.B., Gorski, R.A., and Swanson, L.W. Neurotransmitter specificity of cells and

fibers in the medial preoptic nucleus: an immunohistochemical study in the rat. *J. Comp. Neurol.* 246: 343-363, 1986.

Simerly, R.B., and Swanson, L.W. The organization of neural inputs to the medial preoptic nucleus of the rat. *J. Comp. Neurol.* 246: 312-342, 1986.

Smithson, K.G., Cobbett, P., MacVicar, B.A., and Hatton, G.I. A reliable method for immunohistochemical identification of Lucifer Yellow injected peptide-containing mammalian central neurons. *J. Neurosci. Methods* 10: 59-69, 1984.

Swanson, L.W., and Mogenson, G.J. Neural mechanism for the functional coupling of autonomic, endocrine and somatomotor responses in adaptive behaviors. *Brain Res. Rev.* 3: 1-34, 1981.

Tasker, J.G., and Dudek, F.E. Electrophysiological properties of neurons in the region of the paraventricular nucleus in slices of the rat. *J. Physiol.* 434, 271-293, 1991.

Tasker, J.G., Hoffman, N.W., and Dudek, F.E. Comparison of three intracellular markers for combined electrophysiological, morphological and immunohistochemical analyses. *J. Neurosci. Methods* 38: 129-143, 1991.

van den Pol, A. N., Wuarin, J.-P., and Dudek, F.E. Glutamate, the dominant excitatory transmitter in neuroendocrine regulation. *Science* 250: 1276-1278, 1990.

van Gemert, M., Miller, M., Carey, R.J., and Moses, A.M. Polyuria and impaired ADH release following medial preoptic lesioning in the rat. *Am. J. Physiol.* 228:1293-1297, 1975.

FIGURE LEGENDS

Figure 1. A schematic diagram of the hypothalamic slice preparation containing the medial preoptic area. Abbreviations: ac = anterior commissure, f = fornix, ic = internal capsule, MPA = medial preoptic area, MPN = medial preoptic nucleus, ox = optic chiasm, SDN-POA = sexually dimorphic nucleus of preoptic area, 3V = third ventricle. Adapted from the atlas of Palkovits and Brownstein (1988).

Figure 2. Morphology of a bipolar medial preoptic neuron. Camera lucida drawing (top) and photomicrographs (bottom) showing a biocytin-injected neuron with 2 primary dendrites. As shown at lower power (left), this cell was situated in the sexually dimorphic nucleus of the preoptic area. Calibration bars = 50 μm; iii = third ventricle.

Figure 3. Morphology of a multipolar medial preoptic neuron. Camera lucida drawing (right) and photomicrographs (center and left) showing a biocytin-injected neuron with a multipolar array of primary dendrites. This neuron was located in the medial preoptic nucleus medialis (lower power photomicrograph). Calibration bars = 50 μm; iii = third ventricle.

Figure 4. Schematic diagram of the approximate locations of recorded and stained neurons with respect to medial preoptic subdivisions. A-D represents a rostral-caudal progression through the medial preoptic area (MPOA). Stained neurons are schematicized in terms of

their numbers of primary dendrites. Other abbreviations: ac = anterior commissure; ADP = anterodorsal preoptic nucleus; AVP = anteroventral periventricular nucleus, BST = bed nucleus of the stria terminalis; BSTenc = BST encapsulated portion; DBB = diagonal band of Broca; LPOA = lateral preoptic nucleus; MPNm = medial preoptic nucleus medialis; MePO = median preoptic nucleus; ox = optic chiasm; PVN = paraventricular nucleus; PSCN = preoptic suprachiasmatic nucleus; SDN = sexually dimorphic nucleus of the preoptic area; SCN = suprachiasmatic nucleus; SO = supraoptic nucleus; iii = third ventricle. Schematics were adapted with permission from Simerly and Swanson (1986).

Figure 5. Axon collaterals from a medial preoptic neuron. Camera lucida drawing and photomicrograph of a bipolar neuron located in the sexually dimorphic nucleus of the preoptic area. Note that its axon (a) arose from a primary dendrite (d) and ramified locally. Axon collaterals were covered with varcossities (arrowheads). Calibration bars = 50 μm; iii = third ventricle.

Figure 6. Low-threshold potentials recorded in medial preoptic neurons. A: At rest a neuron fired a single action potential in response to the injection of a depolarizing current pulse (left). As a neuron was hyperpolarized with steady (DC) current, the same intensity current pulse triggered a regenerative depolarization to Na^+-spike threshold, resulting in a short burst of action potentials (middle). The size of this depolarization increased with increasing DC hyperpolarization, shown here during bath application of tetrodotoxin (TTX: 0.5 μg/ml) to a different neuron to block the channels for the fast Na^+ spikes (right). B:

Progressively increasing depolarizing current-pulse intensities from a hyperpolarized condition also progressively increased the size of the low-threshold potential (calibration bars in B also apply to A). C: Time dependence of low-threshold potentials. Hyperpolarizing current pulses had to be sufficiently long for a low-threshold spike to occur with the offset of the pulse, whether the Na^+ spikes were unblocked (left) or blocked (right) with TTX. D: An anode-break spike could generate a burst of Na^+ spikes, and a post-burst afterhyperpolarization could then trigger a membrane oscillation (or series of oscillations) (voltage trace in D is the average of 4 traces). In this and subsequent figures top traces are current, the bottom traces are voltage, and dotted lines indicate resting potential. Traces in B and C (right) are from a female rat.

Figure 7. Effect of Ni^{2+} on low-threshold potentials. When hyperpolarized with steady (DC) current, a depolarizing current pulse of sufficient intensity activated a low-threshold potential, which generated a short burst of Na^+ spikes in normal medium. The low-threshold potential persisted during bath application of tetrodotoxin (TTX: 0.5 μg/ml) but was reversibly blocked by bath application of Ni^{2+} (500 μM) in a low-Ca^{2+} HEPES buffer that also contained TTX. Resting potential (Vr) = -56 mV.

Figure 8. I-V relations of medial preoptic neurons. A: Voltage deflections of a medial preoptic cell in response to current injections. B (left): I-V plots of several representative medial preoptic neurons. Both A and B (left) show linear I-V relations in the hyperpolarizing direction. B (right): I-V plots from the only 2 neurons with non-linear I-V

relations suggesting inward rectification in the hyperpolarizing direction. Traces in A are the average of 4-7 traces except that indicated by the arrowhead, which was averaged across 22 traces for membrane time constant measurement (Fig. 9).

Figure 9. Membrane time constant of a medial preoptic neuron [linearized slope of $(V_0-V_t)/V_0$ plotted against time]. The membrane time constant was from the voltage trace indicated in Fig. 8. The membrane time constant value (τm) shown here was representative of values obtained from all medial preoptic neurons (mean $\pm$ SEM = 15.2 $\pm$ 2.5 ms). Also representative was the presence of an equalizing time constant (τe).

Figure 10. Spike trains in response to different intensities of depolarizing current pulses. In this cell, as in most medial preoptic neurons, spike frequency increased with increasing depolarizing current-pulse intensities, and Na^+ spikes typically showed moderate spike-frequency adaptation across the duration of the pulse. Afterhyperpolarizations usually followed Na^+-spike trains of sufficient frequency (dotted line indicates resting potential).

Figure 11. Evoked and spontaneous postsynaptic potentials recorded in medial preoptic neurons. A: In most medial preoptic cells, an EPSP-IPSP sequence could be evoked by extracellular stimulation of the dorsal preoptic region, however, only at certain stimulus intensities. In this neuron, increasing stimulus intensity only slightly increased IPSP amplitude until an intensity was reached that evoked an EPSP-IPSP sequence (voltage traces are averaged across 4 traces). B: In a few medial preoptic cells, extracellular stimulation of

the dorsal preoptic region evoked one or more IPSPs. The four traces are from the same neuron, where multiple IPSPs were evoked by the same intensity stimulus (30 μA). Note that depolarizations generating action potentials (clipped in this figure) occasionally followed the large IPSPs. C: Spontaneous PSPs, including IPSPs, were frequently recorded in medial preoptic neurons, shown here by four separate traces from the same cell recorded at rest. Arrowhead in A and B indicates stimulus artifact.

Figure 12. Properties of evoked IPSPs. A: In this medial preoptic neuron, a 300 μA extracellular stimulus to the dorsal preoptic region evoked an EPSP-IPSP complex. The IPSP reversed near -72 mV. B: In another medial preoptic cell, a 200-300 μA stimulus to the dorsal preoptic region evoked only an IPSP (top) in normal medium. Bath application of the $GABA_A$ antagonist, bicuculline (BIC, 10 μM) blocked the evoked IPSP, thus revealing an evoked EPSP (middle). The effect of bicuculline was reversible (bottom) and was not accompanied by appreciable changes in input resistance (right traces). During this experiment, the cell was hyperpolarized with 11 pA of steady current to prevent spontaneous firing. Voltage traces in B are averaged across 21-30 individual traces. Arrowheads indicate stimulus artifacts.

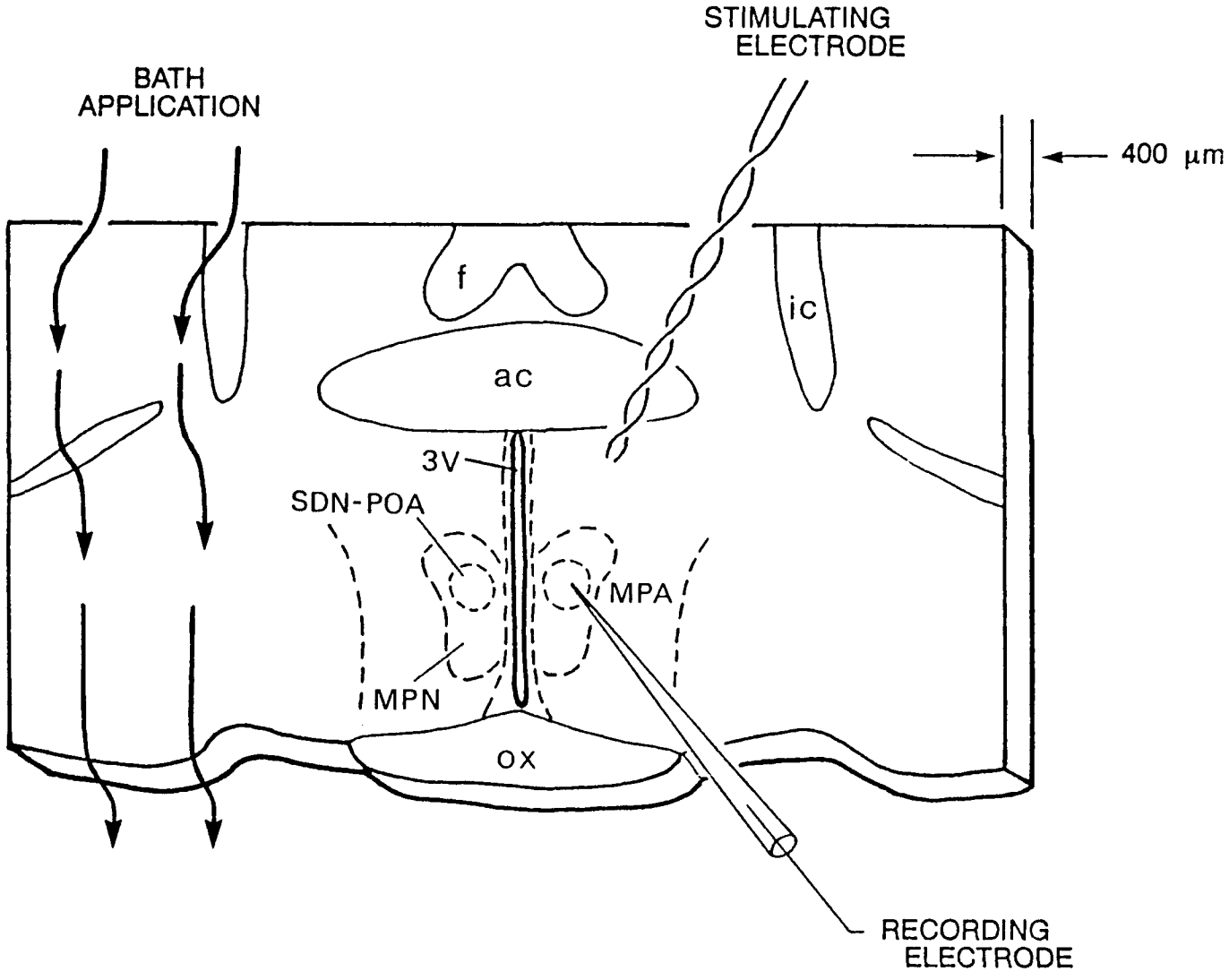
STIMULATING
ELECTRODE
BATH
APPLICATION
400 µm
f
ic
ac
3V
SDN-POA
MPA
MPN
ox
RECORDING
ELECTRODE

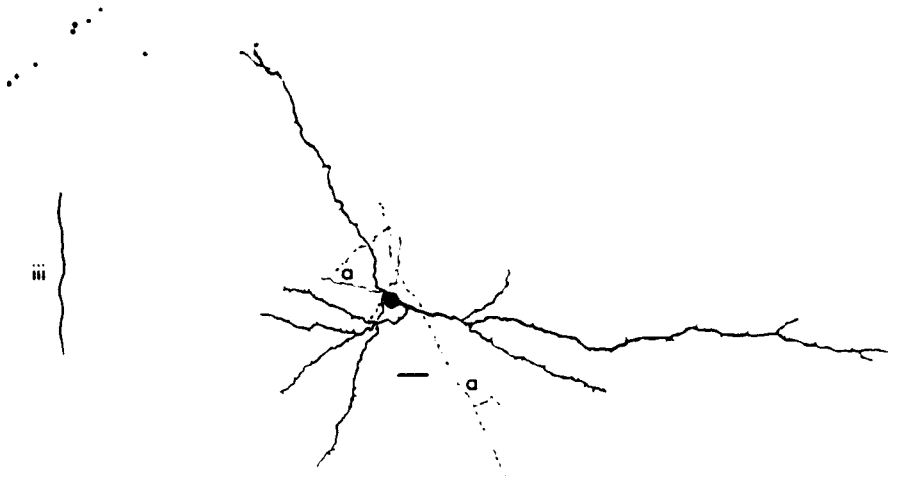
iii
a
a

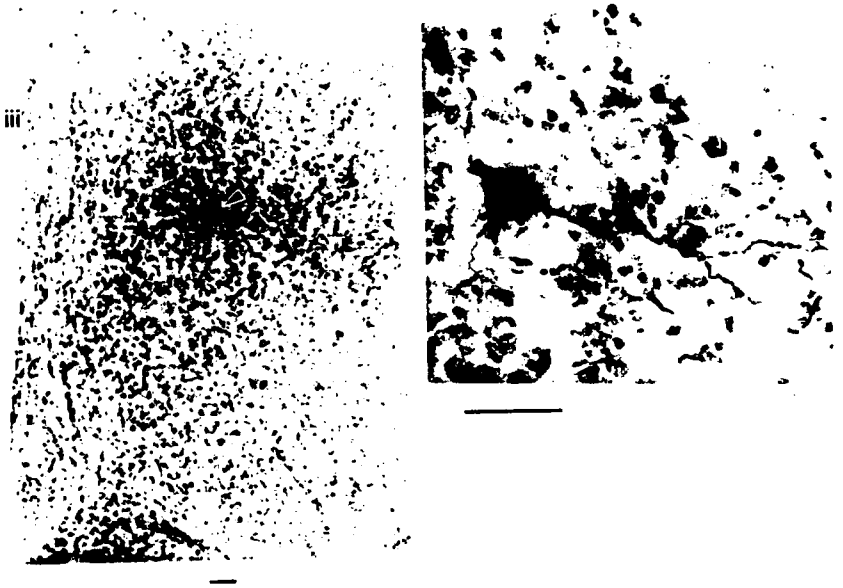
iii

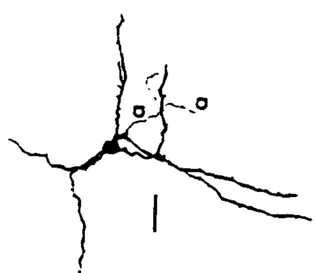

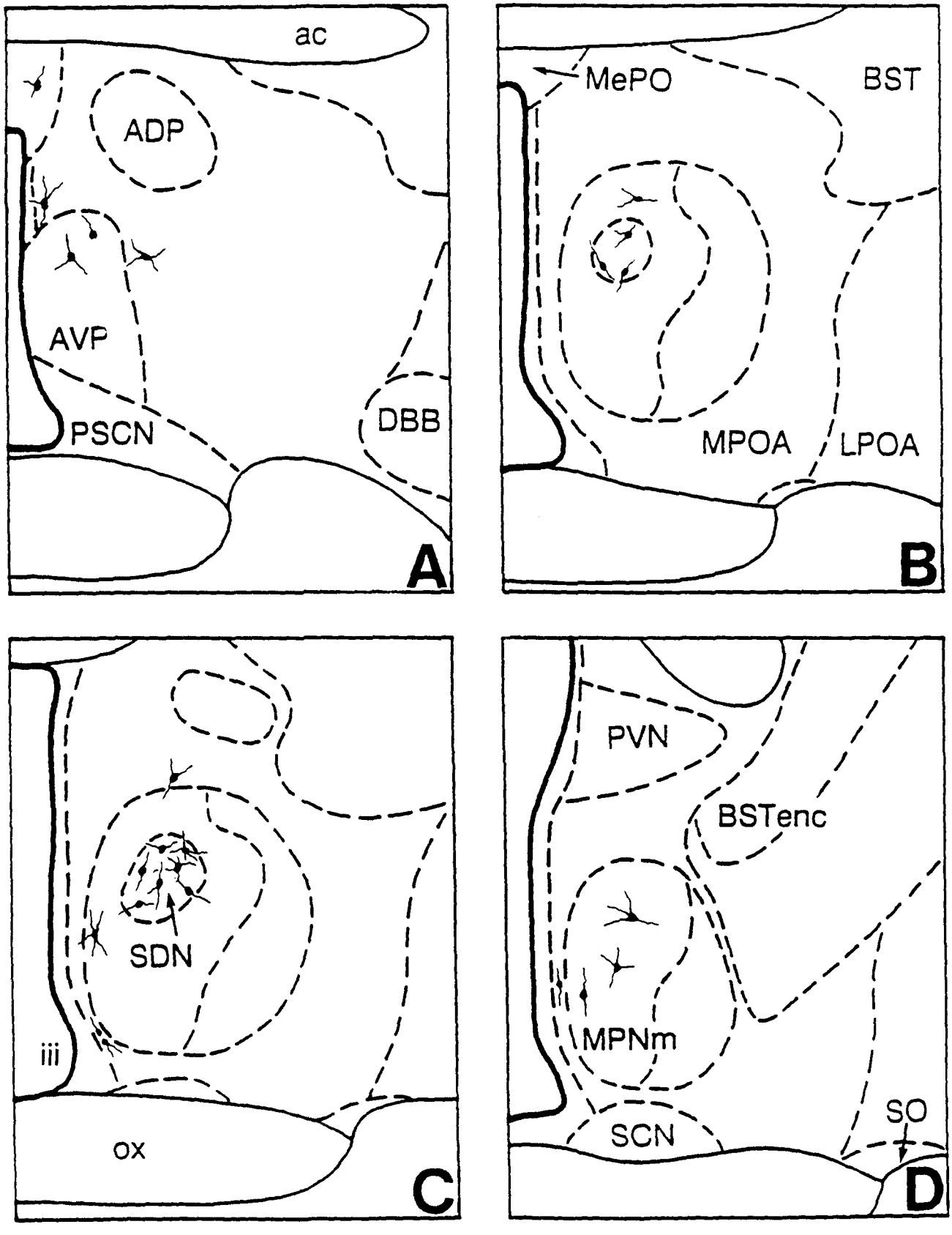
ac
ADP
AVP
PSCN
DBB
A
MePO
BST
MPOA
LPOA
B
SDN
iii
ox
C
PVN
BSTenc
MPNm
SCN
SO
D

Fig. 4


iii
a
a
d
a

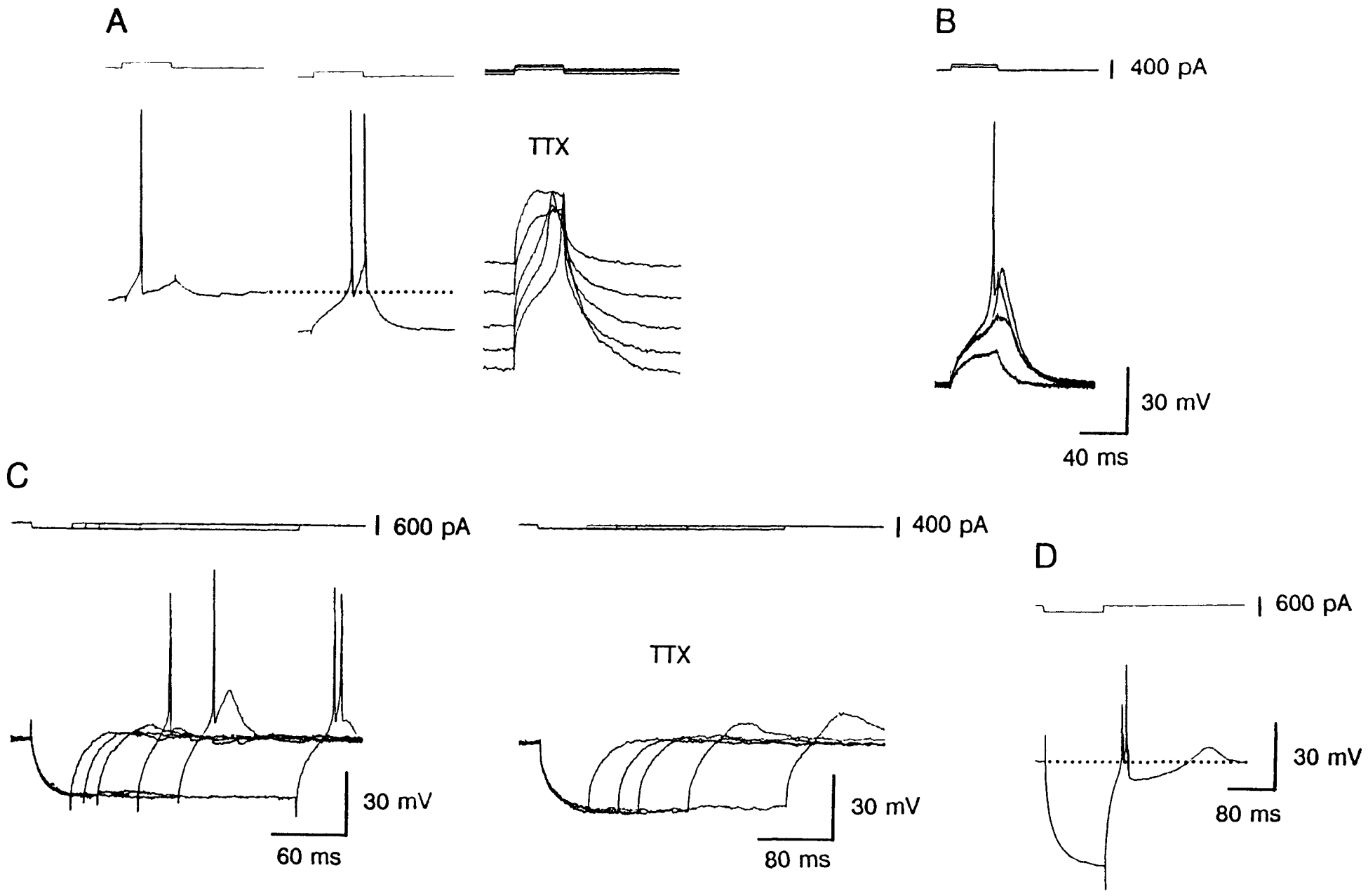
A
TTX
B
400 pA
30 mV
40 ms
C
600 pA
400 pA
30 mV
60 ms
TTX
30 mV
80 ms
D
600 pA
30 mV
80 ms

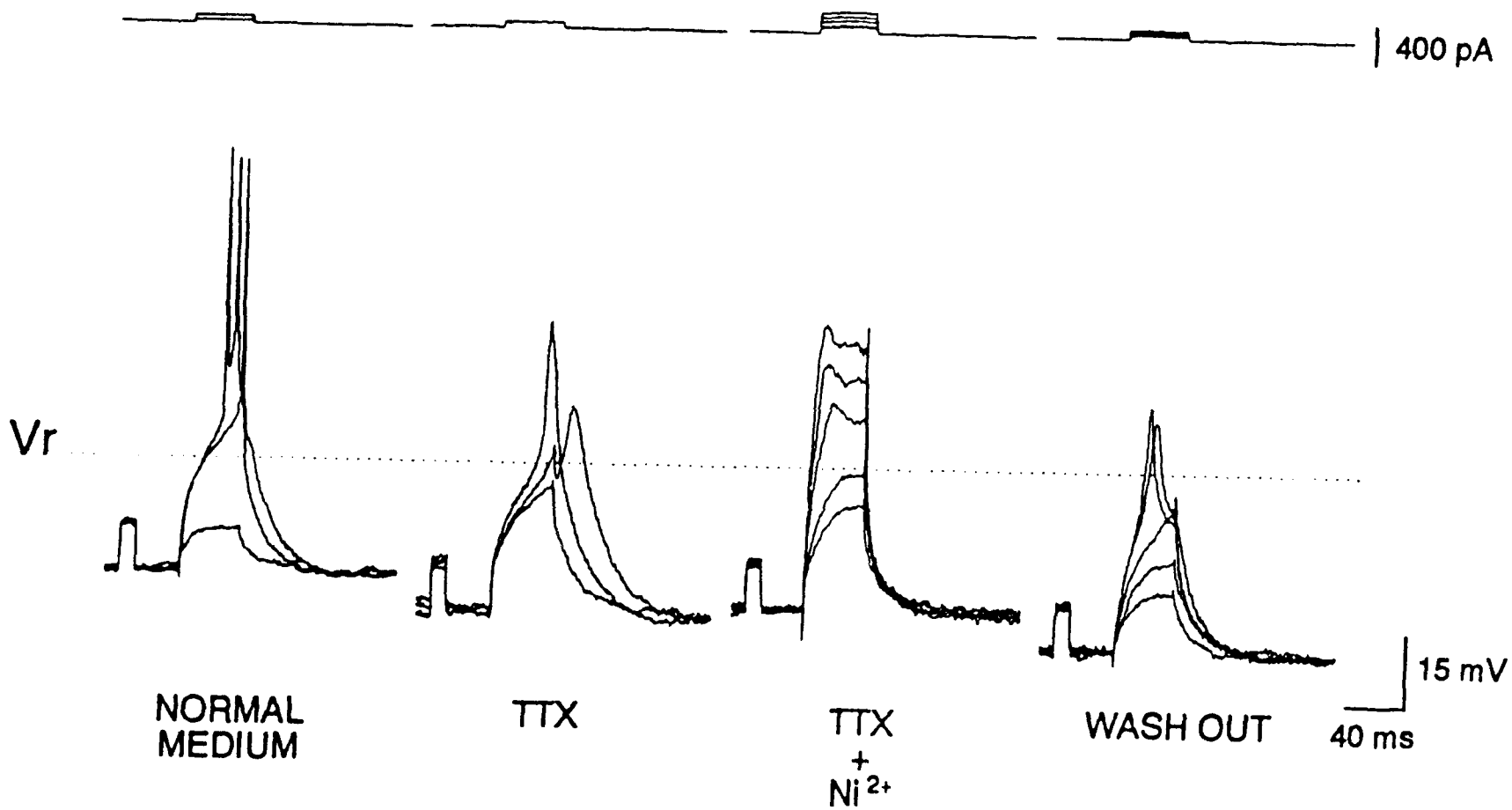
400 pA
Vr
15 mV
40 ms
NORMAL MEDIUM
TTX
TTX + Ni 2+
WASH OUT

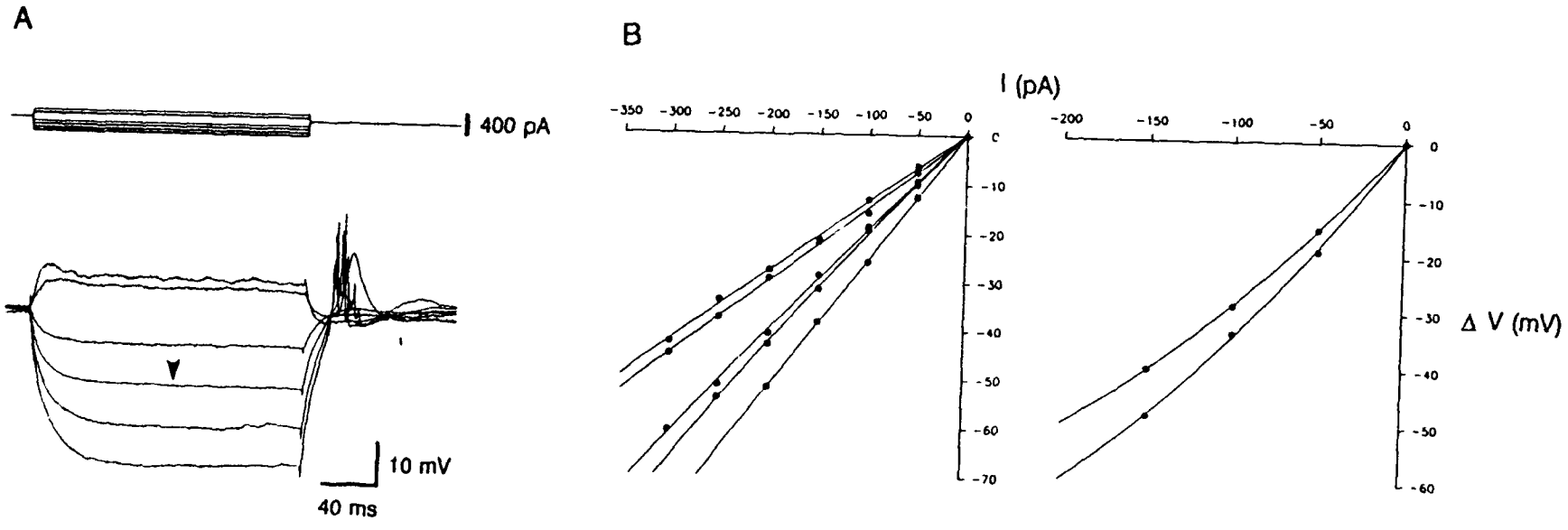
A
400 pA
10 mV
40 ms
B
I (pA)
-350 -300 -250 -200 -150 -100 -50 0
0 -10 -20 -30 -40 -50 -60 -70
-200 -150 -100 -50 0
0 -10 -20 -30 -40 -50 -60
Δ V (mV)

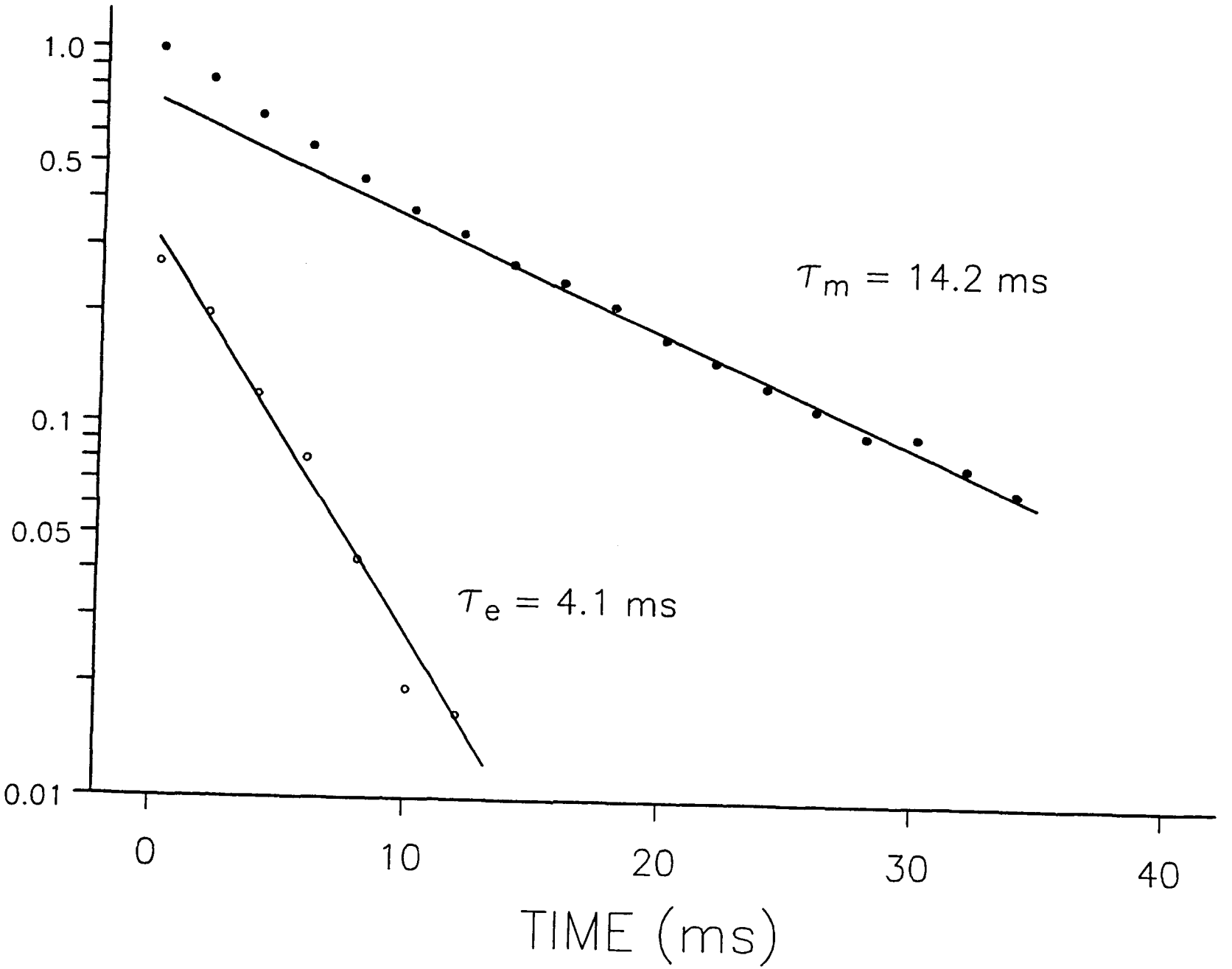
1.0
0.5
0.1
0.05
0.01
τ_m = 14.2 ms
τ_e = 4.1 ms
0
10
20
30
40
TIME (ms)

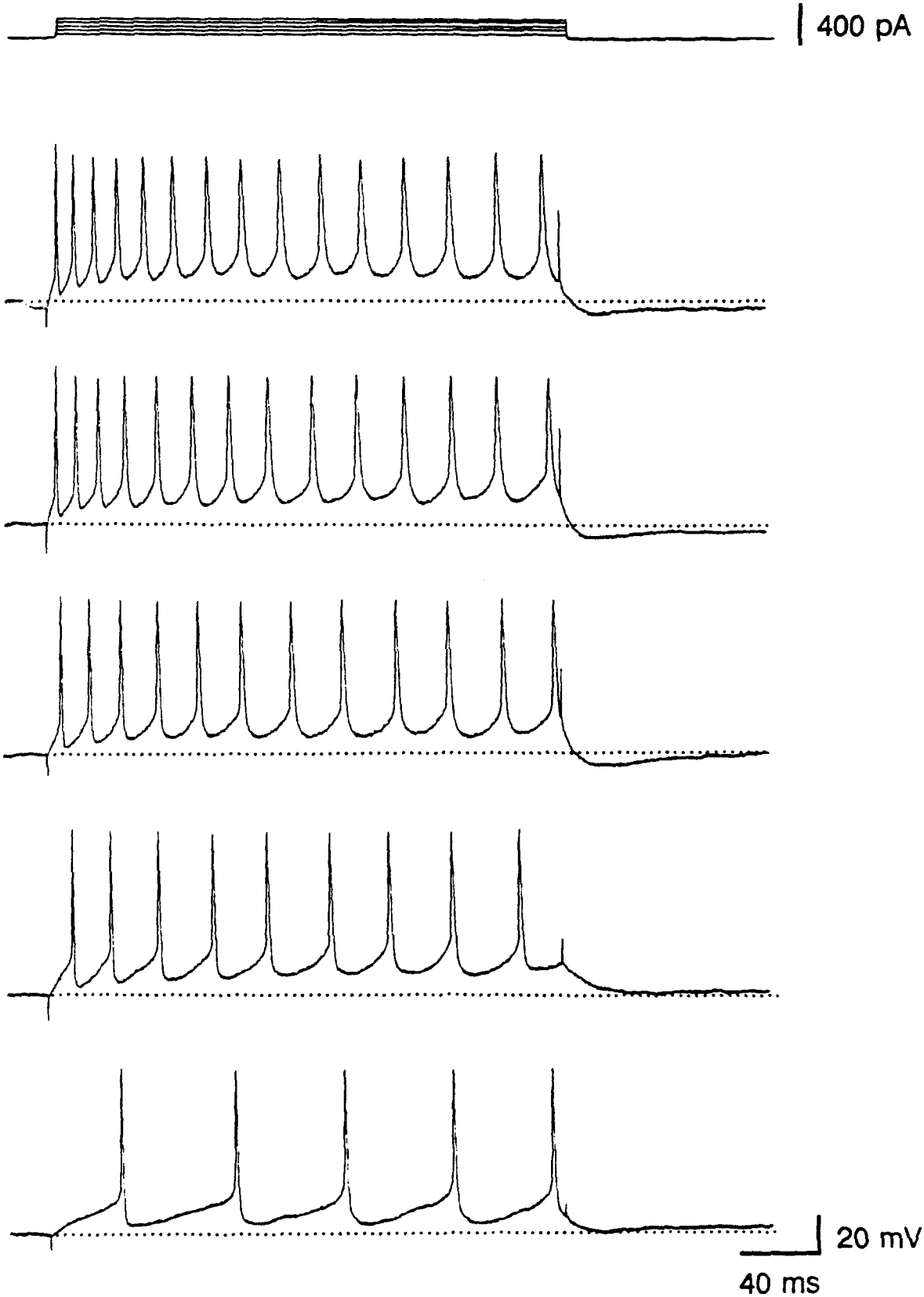
400 pA
20 mV
40 ms

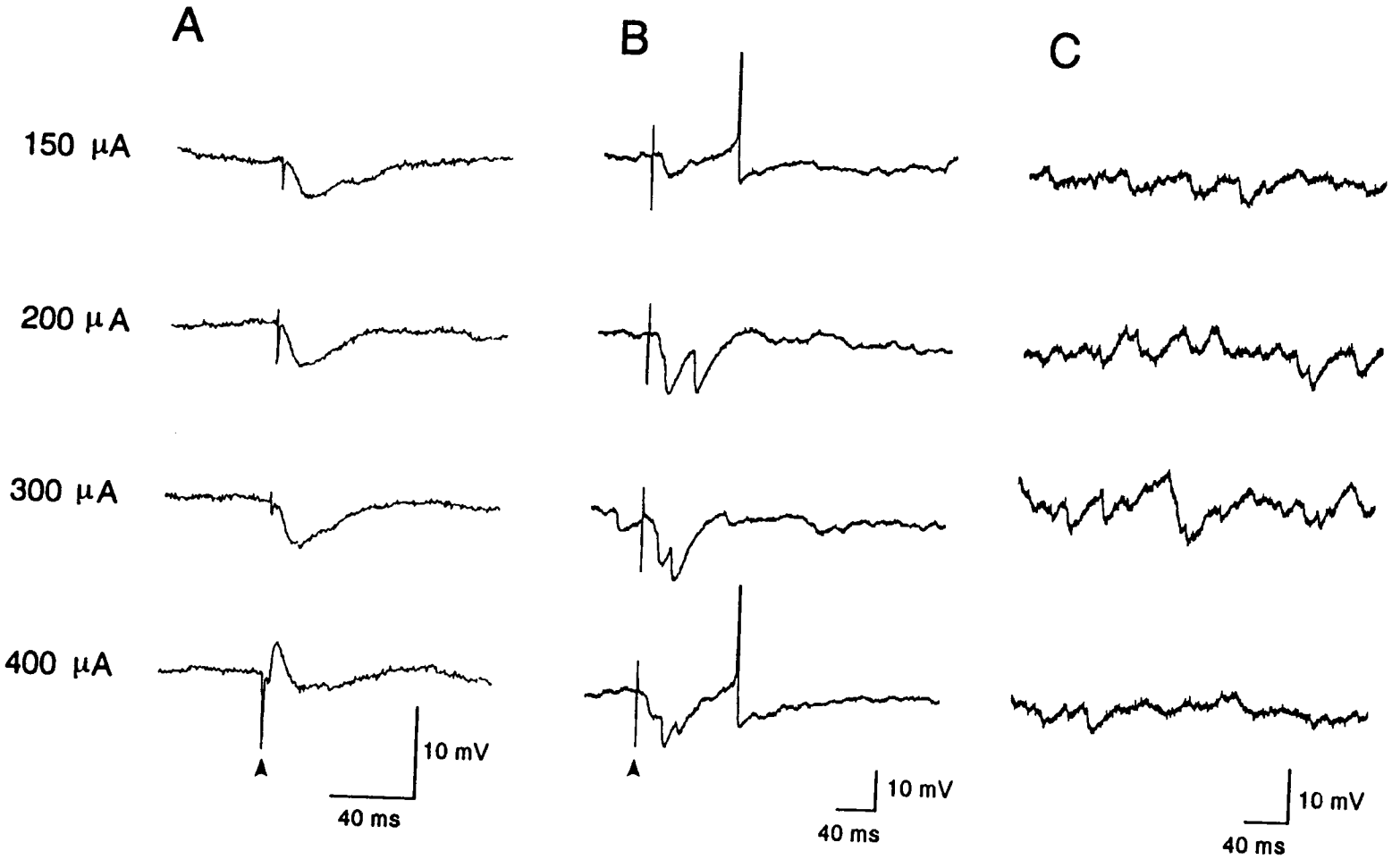
A
B
C
150 μA
200 μA
300 μA
400 μA
10 mV
40 ms
10 mV
40 ms
10 mV
40 ms

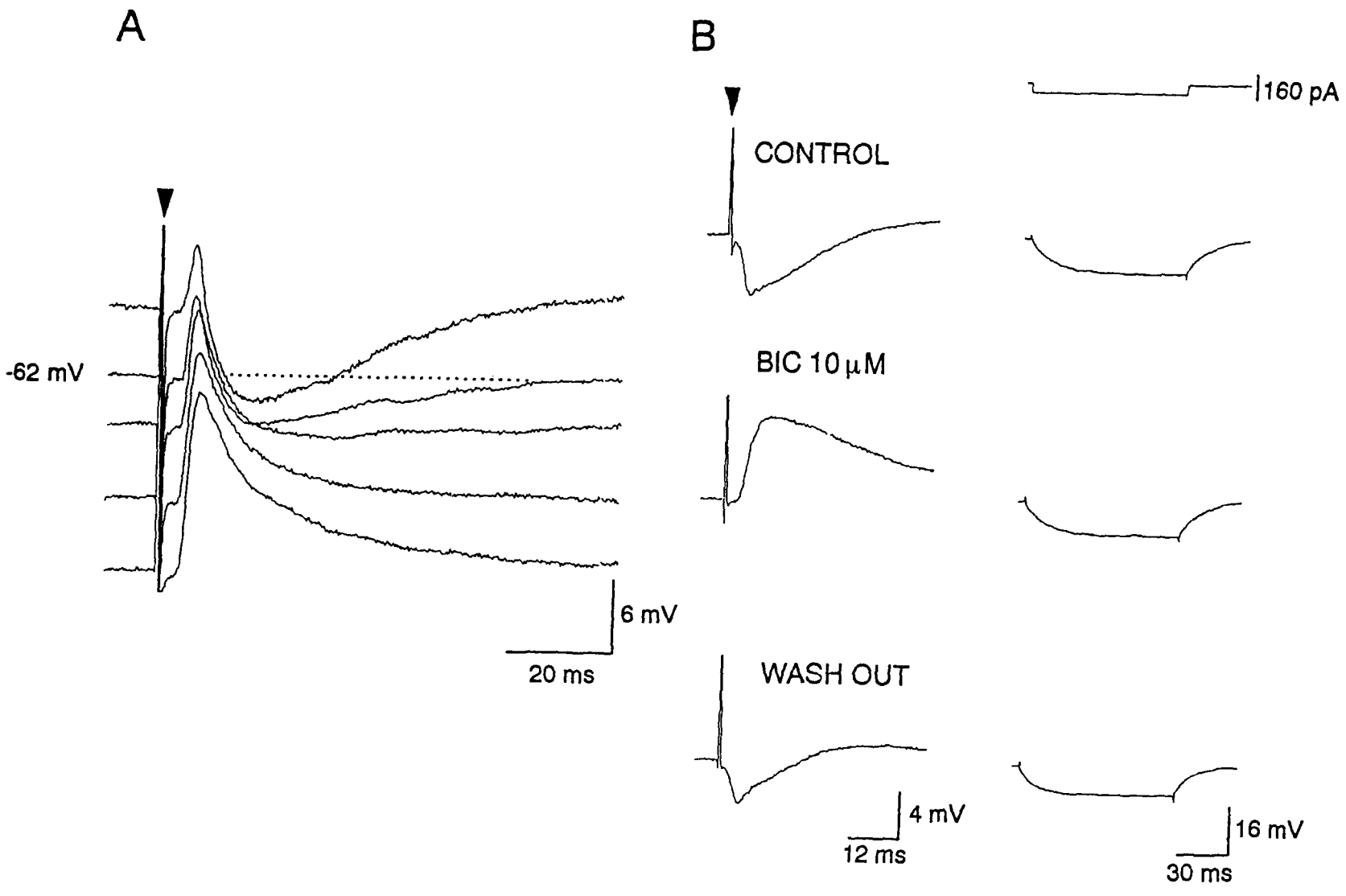
A
B
-62 mV
6 mV
20 ms
160 pA
CONTROL
BIC 10 μM
WASH OUT
4 mV
12 ms
16 mV
30 ms